

NGC 2366 : An optical search for possible supernova remnants [☆]

E. N. Ercan¹

Department of Physics, Bogazici University, Istanbul, 34342, Turkey

E. Aktekin¹

Currently Self-Employed, 1728 Street, Muratpasa, Antalya, 07058, Turkey

Abstract

The results of an optical search for supernova remnants (SNRs) in the nearby irregular galaxy NGC 2366 are presented. We took interference filter images and collected spectral data in three epochs with the f/7.7 1.5 m Russian Turkish Telescope (RTT150) at TÜBİTAK National Observatory (TUG) located in Antalya, Turkey. The continuum-subtracted H α and continuum-subtracted [S II] $\lambda\lambda$ 6716, 6731 images and their ratios were used for the identification of SNRs. With [S II]/H α \geq 0.4 criteria, four possible SNR candidates were identified in NGC 2366 with [S II]/H α ratios of \sim (0.68, 0.57, 0.55 and 0.75), H α intensities of \sim (2.10, 0.36, 0.14, 0.11) $\times 10^{-15}$ erg cm⁻² s⁻¹ [S II] λ 6716/ λ 6731 average flux ratios of \sim (1.01 and 1.04), electron densities of $N_e \sim$ (582 and 513) cm⁻³ and [O III] λ 5007/H β λ 4861 \sim (3.6 and 2.6) line ratio values are obtained for two of the SNR candidates. A shock velocity V_s of $80 \leq V_s \leq 100$ km s⁻¹ is reported. The spectral parameters are obtained for the first time for these possible SNR candidates. The locations of the four SNRs obtained here are found to be consistent with optical and radio results reported so far. One of the sources categorised earlier by *XMM-Newton* observations as an extended X-ray source position is found to be consistent with one of four possible SNR

[☆]Fully documented templates are available in the elsarticle package on CTAN.

¹ercan@boun.edu.tr

²aktekinebru@gmail.com

candidates reported here.

Keywords: ISM: supernova remnants - galaxies: irregular -
galaxies: individual: NGC 2366 - galaxies.

1. Introduction

Supernova explosions and their final dispersion of ejected material have the effect of supplementing the interstellar medium (ISM) with the material produced in stellar interiors and therefore supernova remnants (SNRs) are important for many of the theories of the ISM. Due to the strong photoionisation flux of the central hot star or stars, sulfur is in the form of S^{++} in H II regions, where the $[S II]/H\alpha$ ratio is typically $\approx 0.1 - 0.3$. Outside an H II region, there are not sufficient energetic free electrons to excite S^+ and to give rise to the forbidden-line ($[S II]\lambda 6716, 6731$) emission. Almost all discrete emission nebulae outside H II regions showing $[S II]$ -emission are shock-heated and they are probably SNRs and are characterized by $[S II]/H\alpha \geq 0.4$.

Several early studies discussed the reasons and importance of searching SNRs in nearby galaxies [see e.g. 37, 44, 45] and in our Galaxy [see e.g. 38, 16, 17]. Although there are a large number of Galactic SNRs, the interstellar extinction and uncertain distances cause selection effects. However, in extragalactic samples, these difficulties are much less. All the SNRs in a galaxy are at the same distance from us. Assuming that we know the distance of this galaxy, the properties of these SNRs can be compared directly. In addition, in an extragalactic survey the foreground extinction is generally low such that the relative positions of SNR samples can be determined precisely. The distributions of the SNRs relative to the H II regions in the spiral arms of the Galaxy are calculated using the location of SNRs. Possible SNR progenitors have been searched from these distributions as indicated by Matonick and Fesen [37] and Blair and Long [1, 2]. Extragalactic searches for SNRs were first carried out for the Magellanic Clouds by Mathewson and Clarke [36]. They were the first to use the $[S II]/H\alpha$ emission line ratios for optical identification of SNRs. Blair et al. [3], Smith

et al. [55], Blair and Long [1, 2], Sonbas et al. [57, 58] and Leonidaki et al. [32] have already discussed the motivation for observing SNRs in nearby galaxies based on the same emission-line ratio criterion. Radio searches for extragalactic SNRs have been conducted by Lacey et al. [30], Lacey and Duric [29], Hyman et al. [23]. SNR surveys have also been carried out at optical, radio, and X-ray wavelengths by Pannuti et al. [44, 45, 46].

In this work, we searched for SNRs in the nearby dwarf, irregular galaxy NGC 2366 using the criterion $[S II]/H\alpha$ ratio ≥ 0.4 . It is described as a “cometary” galaxy by Loose and Thuan [33]. Karachentseva et al. [26] reported its distance to be $D=3.44$ Mpc, which is consistent with Tikhonov et al. [63] who reported $D=3.4$ Mpc. The optical and radio studies by Kennicutt et al. [27] showed evidence of very large H II regions in NGC 2366. From the emission-line spectrum of this galaxy, it was found to be exceptional due to its excessively high degree of excitation together with a very low reddening. The authors attributed these features to a very low metal abundance, suggesting the existence of an exceptionally energetic source of ionization. Its 21 cm distinctive spectrum and large scale H II regions are reminiscent of the more distant narrow-lined Markarian galaxies and isolated extragalactic H II regions. Yang et al. [66] have detected 5 $H\alpha$ sources with broad velocity profiles compared to those of their surrounding H I regions. This galaxy is also classified as a dwarf blue galaxy, showing indications of spiral arm structure at several wavelengths [10]. It is dominated in $H\alpha$ by the huge extragalactic H II region in its south west part as indicated by Chu and Kennicutt [8]. Thuan and Izotov [61] provided its V and I photometric results by resolving stars with Wide Field Planetary Camera 2 images obtained from the Hubble Space Telescope (HST). Their 23.65 magnitude limit of the red giant branch stars with ages of > 1 Gyr provided another distance estimate of 3.42 ± 0.15 Mpc which shows a good agreement with the aforementioned values. Early abundance measurements have been reported for this galaxy by several studies [34, 18, 40]. Roy et al. [51, 52] suggested the existence of an expanding supernova bubble in NGC 2363 which is, in fact, a giant H II region within NGC 2366. Its early radio observations were reported by Kennicutt et al.

[28] at $\lambda 6.3$ and $\lambda 2.8$ cm. The authors measured the whole galaxy (in low resolution) and obtained 10 ± 1 mJy flux at 6.3 cm. Their measurement of only the giant H II region at $2''$ resolution yielded 8.5 ± 0.28 mJy flux at $\lambda 6.3$ cm. The difference reported in their spectral indices between the entire galaxy and the giant H II region was attributed to the probable dominant thermal emission across the galaxy. Also Chomiuk and Wilcots [7] reported radio emission of NGC 2366 from VLA continuum data. They diagnosed a number of discrete sources and categorized them as possible SNRs, H II regions, and/or background radio galaxies. Their findings were in good agreement with various studies and with four SNR candidates in NGC 2366 we report here (see our Fig. 1).

Use of the multiwavelength observations is a great help when trying to understand the characteristics and physical parameters of SNRs as has been pointed out by various studies [see e.g. 37, 31, 62].

In the earliest photometric studies, NGC 2366 is described as a nearby galaxy with intense and rare star forming bursts characteristic for evolution of late-type dwarf galaxies [53]. Jaskot and Oey [25] and Micheva et al. [39] also reported this galaxy in their study of the most extreme so-called Green Peas galaxies with the highest [O III]/[O II] ratios. Their [O III] $\lambda\lambda 5007, 4959/\lambda 4363$ ratios yielded electron temperatures of $T_e \sim 15\,000$ K while their [S II] $\lambda 6716/\lambda 6731$ ratios provided electron densities of $N_e = 100\text{--}1000$ cm $^{-3}$ in NGC 2366. $T_e \sim 15\,000$ K was reported for nebular emission by several authors [18, 56]. Gonzalez-Delgado et al. [18] also reported an electron density of $N_e = 235 \pm 41$ cm $^{-3}$. Recently, Vučetić et al. [65] reported their photometric observational results for NGC 2366 and suggested the presence of 67 possible H II regions and two optical SNR candidates.

Thuan et al. [62] report the *XMM-Newton* results of NGC 2366 indicating the existence of two faint X-ray point sources and two faint extended sources. These authors assigned one of these point sources to a possible background active galactic nucleus (AGN), while the other source was found to be coincident with a very luminous star and a compact H II region. Their two faint extended sources were reported to be possibly associated with massive H II regions. An-

other study by Stevens and Strickland [59] was the first *ROSAT* PSPC survey of Wolf-Rayet (WR) galaxies, including NGC 2366. In their study, NGC 2366 was described as a dwarf starburst barred spiral galaxy with an AGN. NGC 2366's *ROSAT* PSPC X-ray position was found to be RA(J2000)=07^h28^m24^s, Dec.(J2000)=69°11'0". These authors traced out WR galaxies and made a possible detection of WR stars in NGC 2363 as was earlier reported by Drissen et al. [12]. Gonzalez-Delgado et al. [18] presented an optical study of NGC 2363 and found broad emission lines at $\lambda 4660$ and $\lambda 5810$ Å indicating the presence of WR stars. They reported a combined mass of these stars of $3.4 \times 10^5 M_{\odot}$, suggesting the existence of a strong outflow, possibly due to the blow-out of a superbubble. Radio observations with lower resolution suggested the emission from NGC 2366 as a whole should be dominated by thermal emission [66]. Stevens and Strickland [59]'s conclusion was that they detected an extended region, however rather with ambiguity. They provided an optical image superimposed with X-ray contours, pointing to a faint extended X-ray emission coming from the nearby star-forming region in NGC 2363 with a contour level of 2.8×10^{-3} count s⁻¹ arcmin⁻². They also found an X-ray point source that might be associated with NGC 2366. The X-ray point source was too faint to obtain a proper spectral fit, but in order to provide its X-ray luminosity they fitted a spectral model with a temperature of $kT = 0.52$ keV, a metallicity of 0.1 Z_{\odot} , and a column density of 4.52×10^{20} cm⁻². With this fit, they obtained an unabsorbed X-ray luminosity of 6.61×10^{37} erg s⁻¹. However, they argued that it could be an underestimation of the real X-ray luminosity in case the actual galactic column density was higher. Therefore, they did not report best-fit values for their analysis. We will compare our possible SNR candidates locations obtained in this work with their corresponding X-ray positions.

Here, we report a detailed study of optical CCD imaging and spectroscopic analysis of NGC 2366. Since there were no X-ray data available other than those summarised here obtained by several authors as indicated above, we could not perform any X-ray data analysis and therefore could not report them here but rather we made some comparison with possible SNR locations obtained in this

Table 1: NGC 2366 properties.

Parameters	Value	References
Morphological Type	IB(s)m	Herrmann et al. 21
Position (J2000)	$RA(J2000) : 07^h 23^m 51^s .85$	Cotton et al. 9
	$Dec.(J2000): Dec.(J2000)=69^\circ 12' 31'' .10$	
Redshift	0.000330	Paturel et al. 47
Distance	3.44 Mpc	Tolstoy et al. 64
Diameter	7.36 kpc	★
B-band effective radius consistent with Lyman-break analogs	$r_{1/2} = 2.7 \pm 0.1$ kpc	Hunter et al. 22

★: <http://annesastronomynews.com/photo-gallery-ii/galaxies-clusters/ngc-2366/>

work and the early limited X-ray results published so far.

Our work is structured as follows. The description of the observations and data reduction is given in Section 2. Our discussion and conclusions can be found in Section 3. The fundamental physical properties of NGC 2366 are given in Table 1.

2. Observations and Data Reduction

The observations are performed in three different epochs by using the Russian-Turkish–Telescope (RTT150)³. The first epoch is on 29th of March 2017 (CCD1), the second epoch is on 23rd - 24th of December 2017 (CCD2) and the third epoch is on 9th - 10th September 2018 (CCD2). The seeing conditions were consistent throughout the whole observations within a range of 1.8–2.0 ″.

2.1. Imaging observations

The RTT150 has a Ritchey-Chrétien optical system functioning together with Cassegrain and Coude focal systems. We used a TFOSC-CCD, with the

³Specifications of RTT150 and TÜBİTAK Faint Object Spectrometer and Camera (TFOSC) are available at <http://www.tug.tubitak.gov.tr>.

Table 2: Specifications of the CCDs on RTT150 Telescope.

Properties	CCD1	CCD2
Pixel Format	2048 × 2048 pixel	2048 × 2048 pixel
Pixel Sizes	15 μm	13.5 μm
Image View	13.3 × 13.3 arcmin ²	11.3 × 11.3 arcmin ²

Table 3: The filter characteristics and exposure times.

Filter	Wavelength (Å)	FWHM (Å)	Exposure times (s)	Observations date
H α	6563	80	3 × 300	29th March 2017
			6 × 900	23rd - 24th December 2017
			6 × 900	9th - 10th September 2018
H α cont.	6446	123	1 × 300	29th March 2017
			6 × 300	23rd - 24th December 2017
			6 × 300	9th - 10th September 2018
[S II]	6728	54	3 × 300	29th March 2017
			6 × 900	23rd - 24th December 2017
			6 × 900	9th - 10th September 2018
[S II] cont.	6964	350	1 × 300	29th March 2017
			6 × 300	23rd - 24th December 2017
			6 × 300	9th - 10th September 2018

f/7.7 focal ratio Cassegrain low resolution faint object spectrograph and camera throughout our observations. Our imaging observations were completed by using H α , H α cont., [S II] and [S II] cont. narrow band filters. The technical properties of the CCDs (i.e. CCD1 and CCD2) used during our three epochs of observations are given in Table 2. The log of the optical observations are shown in Table 3.

2.2. Imaging data analysis

The raw data was processed by using an Image Reduction and Analysis Facility (IRAF)⁴ for data reduction and also by The European Southern Observatory Munich Image Data Analysis System (ESO-MIDAS)⁵.

Standard procedures were used for data reduction, which include the bias corrections, overscan at field, and cosmic ray elimination by making use of the IRAF CCDPROC package and MIDAS CCDRED application packages. To inspect the locations of the stars, positions of red stars from the USNO A2.0 catalog Monet et.al. [15] were implemented. Fig. 1 presents the positions of the SNR candidates overlaid on the Digitized Sky Survey (DSS)⁶ image of the NGC 2366 galaxy. [S II]-[S II]cont. and H α -H α cont. images were obtained after achieving the second step from the cleaned images. Finally, the [S II]/H α ratio can be reached by forming the ratio of these above mentioned two images. Standard stars Feige34, HR 5501 and HR 8634 [see e.g. 35, 19, 20] were both observed to calibrate its optical flux.

We began the selection process of candidate SNRs in NGC 2366 by constructing continuum-subtracted H α and [S II] $\lambda\lambda$ 6716, 6731 images and calculating the [S II]/ H α image ratios. The regions having image ratio values ≥ 0.4 were identified as candidate SNRs [1].

Preliminary SNR candidates were found by blinking between continuum-subtracted [S II] and H α sub-field images. For visual inspection of the fields to search for candidates, we produced images of a $2' \times 2'$ region. The bright features in the continuum-subtracted [S II] image were checked against the continuum-subtracted H α image to make sure that the stars were not crudely subtracted. If any feature seen on the [S II] image looked brighter than it was in the H α image, we tagged it as a candidate SNR, a possible target for follow-up spectral observations.

⁴developed by USA National Optical Astronomical Observatories (NOAO)-
<https://iraf-community.github.io/>

⁵<http://www.eso.org>

⁶<https://archive.eso.org/dss/dss>

We made use of the [S II], H α images and their continuum-subtracted images to measure the total counts for each candidate SNR. Then a circular aperture in the continuum-subtracted images was chosen to sum the Analogue to Digital Units (ADU) counts. A concentric annulus region was applied to pick the background counts, which were later subtracted from the aperture sum.

The seeing was obtained during interference filter imaging observations (namely, 1.9 '' corresponding to ~ 32 pc for the assumed distance to NGC 2366 of 3.44 Mpc), which is implemented in constraining the aperture sizes used for the measurements of fluxes. We did not include radii calculations for the detected SNR candidates, because of the differences we found between seeing and pixel scales. We used data from Cardelli et al. [5] to correct flux values for interstellar extinction.

Jacoby et al. [24] gave a description of the conversion process from instrumental counts into physical units of ($\text{erg cm}^{-2} \text{s}^{-1}$). Fig. 1 shows the combined three epochs H α image of NGC 2366 with J(2000) coordinates. Detected possible SNR candidates are shown together with their numbers of 1, 2, 3, 4. Individual images in each filter were aligned and combined with the `combine` packages of IRAF and ESO-MIDAS. The combination of these data sets are appropriate for the particular analysis presented in the paper. During these observations two different CCDs were used as can be seen from Table 2. CCD1 and CCD2 have almost identical angular resolution, and their quantum efficiencies are similar to each other as well as their seeing between our three epochs of observation.

To be able to get better statistics and therefore better scientific results, we have decided to combine the imaging data for three epochs with the two CCDs. The possible SNR candidates obtained from the combined data are shown in Fig. 1.

A total of four possible SNR candidates near the central part of the NGC 2366 with appropriate [S II]/H α ratio and three H II regions are suggested by us, from the combined data as shown in our Table 4 and in Fig. 1 top panel.

Table 4: Combined optical imaging data for the four SNR candidates (SNR1, SNR2, SNR3, SNR4), their corresponding radio coordinates reported by Chomiuk and Wilcots [7] of our IDs of SNR1, SNR2, SNR3, SNR4 and three H II regions (1, 2, 3) with their H α fluxes, [S II]/H α ratios and their errors. SNR1, SNR2 and H II 1 correspond here to the two optical SNR candidates and one H II region respectively, as reported by Vučetić et al. [65] and are shown as Vuc5, Vuc34 and Vuc 52.

ID	Optical Coordinates		Radio Coordinates ⁺	[S II] / H α	I (H α) $\times 10^{-15}$ (erg cm ⁻² s ⁻¹)
	<i>RA(J2000)</i>	<i>RA(J2000)</i>	<i>RA(J2000)</i>		
	<i>Dec.(J2000)</i>	<i>Dec.(J2000)</i>	<i>Dec.(J2000)</i>		
SNR1 (Vuc 5)* (Cho 07) ⁺	07 ^h 28 ^m 30 ^s .70 69°11'33"60	07 ^h 28 ^m 30 ^s .41 69°11'33"80		0.68 (± 0.05)	2.10
SNR2 (Vuc 34)* (Cho 15) ⁺	07 ^h 28 ^m 52 ^s .30 69°12'53"00	07 ^h 28 ^m 52 ^s .10 69°12'54"40		0.57 (± 0.04)	0.36
SNR3 (Cho 18) ⁺	07 ^h 28 ^m 57 ^s .50 69°13'41"80	07 ^h 28 ^m 57 ^s .67 69°13'41"00		0.55 (± 0.02)	0.14
SNR4 (Cho 12) ⁺	07 ^h 28 ^m 45 ^s .24 69°12'20"70	07 ^h 28 ^m 45 ^s .26 69°12'19"80		0.75 (± 0.05)	0.11
H II 1 (Vuc*52)	07 ^h 29 ^m 01 ^s 69°13'30"			0.11 (± 0.01)	0.05
H II 2	07 ^h 28 ^m 57 ^s .50 69°13'33"			0.26 (± 0.01)	0.13
H II 3	07 ^h 29 ^m 04 ^s .20 69°13'31"05			0.09 (± 0.01)	0.07

Notes. * From Vučetić et al. [65], + From Chomiuk and Wilcots [7].

2.3. Spectral observations

Our spectral observations were performed by using the Cassegrain-TFOSC / CCD of RTT150. Spectral measurements were obtained in the $\lambda 3230\text{--}9120 \text{ \AA}$ range with the grism G15. In total spectra of 5 different regions have been analysed. For the flux calibration, we have observed the standard stars (Feige34, HR 5501 and HR 8634) as our spectrophotometric standards as suggested by [see e.g. 35, 19, 20]. Fe-Ar calibration lamp frames were obtained for slit width for each observation. High-resolution long-slit spectra of two possible SNR candidates, SNR1 and SNR4, are reported here together with those of three possible detected H II regions (H II-1, H II-2 and H II-3).

2.4. Spectral data analysis

The spectroscopic observations were performed on March 29, 2017 (Epoch 1) and September 9, 2018 (Epoch 3) with the RTT150 using the medium resolution spectrometer TFOSC. The grism G15 with the nominal dispersion of $\sim 8 \text{ \AA pixel}^{-1}$ was used. The reduction and analysis of a spectrum are made using the package Longslit context of IRAF. The exposure time for each spectrum is 3600 s. The slit width we used during our spectral observations was $1.78''$ (100μ). The resolution at $H\alpha$ is 16 \AA .

The ratio $[S II]/H\alpha$ and the electron density are calculated from the $[S II]$ ($\lambda 6716/\lambda 6731$) flux ratios following the work done by Osterbrock and Ferland [41]. Using the $[O III]\lambda 5007/H\beta$ line ratio, the shock velocities, V_s , proposed for extragalactic SNRs are estimated from the study of Matonick and Fesen [37] and the measurements of $[O III]\lambda 5007/H\beta$ ratios reported by Dopita et al. [11] providing an estimate for the $[O III]\lambda 5007/H\beta$ ratio as a function of shock velocity. These authors also provided the plots of this ratio in their Figs 5 and 6 in terms of V_s . Our $[O III]\lambda 5007/H\beta$ ratio range (2.61–3.57) is obtained from our individual spectral analyses for the four SNR candidates and the shock velocities of $H\alpha$ were produced by a dust screen distribution using the relations of Relano et al. [49], Buat et al. [4] as can be seen from Table 5.

The interstellar extinction and the extinction of H α produced by such a dust screen distribution were also determined through the relations of Relano et al. [49], Buat et al. [4] together with Neutral Hydrogen column density relation from Predehl and Schmitt [48]. This is similar to the determinations reported for another nearby galaxy by Ercan et al. [14].

The spectral parameters of SNR1 and SNR4, including the relative line flux and electron density (N_e)⁷ parameter were derived from the [S II]($\lambda 6716/\lambda 6731$) ratios for an assumed electron temperature of 10^4 K [41].

The spectra of our possible candidates SNR1 and SNR4 together with those of the three possible H II regions of 1, 2, and 3 in the range of $\lambda 4500\text{--}7000$ Å, are presented in Table 5 and Fig. 2 and Fig. 3. Our results for SNR1 and SNR2 are found to be consistent with the optical observations reported recently by Vučetić et al. [65]. However, our SNR3, SNR4, H II-2 and H II-3 have not been detected by these authors. The limiting flux sensitivity of our imaging observations is obtained by taking a blank and faintest part in a circle same circular aperture with our 4 SNRs and found to be 0.037×10^{-15} erg cm⁻² s⁻¹. In Drissen et al. [13] NGC 2366BG7, located at $RA(J2000) = 07^h 28^m 45^s.3$, $Dec.(J2000) = 69^\circ 12' 19''.2$ is reported as one of the background galaxies in the direction of NGC 2366 by using MKR 71 and NGC 2363 Hubble Space Telescope (HST) data. Its position is found to be consistent with our SNR4. It is also consistent with one of the five radio SNRs suggested by Chomiuk and Wilcots [7] as their one out of five SNRs so-called Cho 12.

Chomiuk and Wilcots [7] reported radio observations of NGC 2366 and suggested the sources Cho 07, Cho 15, Cho 18 and Cho 12 to be possible SNR candidates. In this study, our possible four SNR candidates (see Table 4) are all found to be in a good agreement with their 20 cm radio locations. Our H II regions reported here are consistent with the findings of Vučetić et al. [65] results.

⁷calculated with The Space Telescope Science Data Analysis System (STSDAS) task `nebular.temden` program; this task is based on the program FIVEL [50, 54] for a five level atom

Table 5: Relative line intensity for the SNR candidates (SNR1 and SNR4). Fluxes are normalised $F(\text{H}\alpha) = 100$. The signal-to-noise ratios (S/N) of the emission lines are given together with other physical parameters.

Lines (\AA)	Fluxes ($\text{H}\alpha=100$) and S/N			
	SNR1		SNR4	
	F	S/N	F	S/N
H β ($\lambda 4861$)	31.36	5	18.70	4
[O III] ($\lambda 4959$)	36.92	5	37.40	9
[O III] ($\lambda 5007$)	111.80	15	48.78	5
[N II] ($\lambda 6548$)	28.25	12	24.39	5
H α ($\lambda 6563$)	100	15	100	18
[N II] ($\lambda 6584$)	43.16	6	32.52	6
[S II] ($\lambda 6716$)	36.97	5	42.28	4
[S II] ($\lambda 6731$)	36.56	5	40.65	4
Parameters & Line Ratios	Values			
I ($\text{H}\alpha$) ($10^{-15} \text{ erg cm}^{-2} \text{ s}^{-1}$)	1.92 ± 0.04		0.12 ± 0.03	
[S II] ^a / H α	0.74 ± 0.11		0.82 ± 0.08	
[S II] $\lambda 6716/\lambda 6731$	1.01 ± 0.08		1.04 ± 0.07	
[O III] ($\lambda 5007$)/H β ($\lambda 4861$)	3.57 ± 0.07		2.61 ± 0.14	
V_s (km s^{-1})	80–100		80–100	
$E(B - V)$	0.36 ± 0.06		0.26 ± 0.07	
$A_{(\text{H}\alpha)}$	0.25 ± 0.06		1.43 ± 0.07	
$N(\text{H I})$ (10^{20} cm^{-2})	2.42 ± 0.05		13.80 ± 0.2	
N_e (cm^{-3})	581.91 ± 168.61		513.38 ± 135.88	

Notes. ^a [S II] is the combination of the $\lambda 6716$ and $\lambda 6731$ flux values.

In order to verify the photometric calibration, H α fluxes of our possible SNR candidates are compared and given in our Table 5. Our flux values are found to be in the range of $(0.11 - 2.10) \times 10^{-15}$ erg cm $^{-2}$ s $^{-1}$. Vučetić et al. [65]’s work of optical imaging observations revealed the existence of two optical SNR candidates together with their characteristics of H α and [S II] fluxes across the two fields of view in NGC 2366. Our SNR1 and SNR2 locations are consistent with their findings. However, our SNR3 and SNR4 are consistent with the radio results given by Chomiuk and Wilcots [7] which may indicate the possible existence of two new optical SNR candidates in NGC 2366.

Vučetić et al. [65] reported 67 possible H II regions in their work and their so-called Vuc 52 is consistent with our H II-1 position as shown in our Table 4. The XMM-Newton X-ray position given at $RA(J2000) = 07^h28^m58^s.2$, $Dec.(J2000) = 69^\circ11'34''$ by Thuan et al. [62] is found to be very close when compared with 5th radio position reported by Chomiuk and Wilcots [7]

3. Discussions and conclusions

In this work, we present an optical study for the SNR candidates using narrow-band images and their spectra obtained with RTT150-TUG for the first time. We have identified four possible SNRs, with appropriate [S II]/H α ratios and three possible H II regions. Our conclusions are;

- (i) From optical imaging, the ratio [S II]/H $\alpha \geq 0.4$ is used in our work to identify the possible SNR candidates. We identified a total of four SNR candidates in NGC 2366 together with a possible existence of three H II regions using our combined optical data. Out of four SNR candidates reported here, the two of them are newly discovered SNR candidates in NGC 2366. New spectroscopic observations of five of these sources (SNRs & H II regions) are presented as well.
- (ii) Spectral analyses are also performed here for two of our possible SNR candidates in NGC 2366. We report the range of line fluxes and the

parameters of $[\text{S II}]/\text{H}\alpha = 0.74 - 0.82$, $[\text{S II}](\lambda 6716/\lambda 6731) = 1.01 - 1.04$, shock wave velocities of $80 < V_s < 100 \text{ km s}^{-1}$, its optical extinction range of $E(B - V) = 0.26 - 0.36$, $A_{(\text{H}\alpha)}$ in the range of 0.25 - 1.43, absorbing column density range of $N(\text{H I}) = (2.42 - 13.80) \times 10^{20} \text{ cm}^{-2}$ and electron density range of $N_e = (513 - 581) \text{ cm}^{-3}$, as shown in Table 5. Two out of four SNR candidate locations reported in this work are found to be consistent with Vučetić et al. [65]’s results. We must point out here that optical flux values we have reported here are found to be consistent with other nearby galaxy SNRs (see e.g. Sonbas et al. [57, 58]. Pakmor et al. [42, 43], Taubenberger et al. [60], Leonidaki et al. [32] are mentioned the spectral features of SNRs in nearby galaxies and the relation with their emission lines. A viable model for normally bright SNe Ia, where nebular O I emission had never been observed could be a similar case that fit with our spectral results presented in this study.

- (iii) According to Chomiuk and Wilcots [7] radio observations, five radio SNR candidates are reported. All of our possible SNR candidates locations presented here are found to be consistent with four of their SNR positions (see our Table 4).
- (iv) The fainter and possibly extended *XMM-Newton* source J072830.4+691132 reported by Thuan et al. [62] coincides with our SNR candidate SNR1 to within about 2", which may suggest its association with a possible SNR candidate when it is considered in junction with our spectral results of SNR1.

Stevens and Strickland [59]’s *ROSAT* PSPC study of NGC 2366 supported the existence of characteristic extended region at $RA(J2000) = 07^h 28^m 24^s$, $Dec.(J2000) = 69^\circ 11' 0''$ which is not exactly coincident with any of our observed possible SNR candidates, studied here. However, it can be considered nearest to our SNR1 candidate at $RA(J2000) = 07^h 28^m 30^s .7$, $Dec.(J2000) = 69^\circ 11' 33'' .60$.

- (v) We must emphasize here that in the X-ray band, NGC 2366 has very limited observations and previous X-ray studies outlined above could not contribute much to the existence of possible SNR candidates in this nearby galaxy. Further deep observations are needed by satellites such as *Chandra* and/or *XRISM* to achieve a better understanding of the X-ray properties of NGC 2366. For this purpose we are in a stage of submitting a *Chandra* proposal for a better understanding of the possible SNR candidates and the physics behind them.
- (vi) About the SN rate, Chakrabarti et al. [6] reported the SN rates are obtained using the data from Lick Observatory Supernova Search (LOSS). The rate beyond the optical radius of spiral galaxies host 2.5 ± 0.5 SNe per millennium. The rates of core-collapse SNe that may collapse to form the massive black holes detected by the Laser Interferometer Gravitational-Wave Observatory (LIGO) in the outer discs of spiral is reported to be 1.5 ± 0.15 per millennium and for dwarf galaxies is 2.6 ± 1.5 SNe per millennium or in otherwords, $31,000 \pm 18,000$ SNe Gpc⁻³ yr⁻¹. The relative ratio of core-collapse to SNe Ia is comparable in the inner and outer parts in dwarf galaxies. There is no SN rate reported . Since there is no reported SN rate for NGC 2366, one can assume that the predicted SNe rate for dwarf galaxies mentioned above may well be applicable for NGC 2366 .

Acknowledgements

We appreciate the valuable comments given by the referee and we thank TÜBİTAK-TUG for their support in using RTT150 (Russian-Turkish Telescope) for our observations performed through Project number 15BRTT150-842. This work is supported by Bogazici University, BAP with project number 8563 and ENE thanks BAP for their support. We thank Dr. Aytap Sezer for many useful discussions and Prof.Dr.Reynier Peletier for his valuable comments.

References

- [1] W. P. Blair and K. S. Long. Identification of supernova remnants in the sculptor group galaxies ngc 300 and ngc 7793. *The Astrophysical Journal Supplement Series*, 108:261–277, 1997. doi: 10.1086/312958.
- [2] W. P. Blair and K. S. Long. An optical survey of supernova remnants in m83. *The Astrophysical Journal Supplement Series*, 155:101–121, 2004. doi: 10.1086/423958.
- [3] W. P. Blair, R. P. Kirshner, and R. A. Chevalier. Supernova remnants in m 31. *Astrophysical Journal*, 247:879–893, 1981. doi: 10.1086/159098.
- [4] V. Buat, A. Boselli, G. Gavazzi, and C. Bonfanti. Star formation and dust extinction in nearby star-forming and starburst galaxies. *Astronomy and Astrophysics*, 383:801–812, 2002. doi: 10.1051/0004-6361:20011832.
- [5] J. A. Cardelli, G. C. Clayton, and J. S. Mathis. The relationship between infrared, optical, and ultraviolet extinction. *Astrophysical Journal*, 345: 245–256, 1989. doi: 10.1086/167900.
- [6] S. Chakrabarti, B. Dell, O. Graur, A. V. Filippenko, B. T. Lewis, and C.F McKee. The supernova rate beyond the optical radius. *The Astrophysical Journal Letters*, 863:L1–L5, 2018. doi: 10.3847/2041-8213/aad0a4.
- [7] L. Chomiuk and E. M. Wilcots. A search for radio supernova remnants in four irregular galaxies. *The Astronomical Journal*, 137:3869–3883, 2009. doi: 10.1088/0004-6256/137/4/3869.
- [8] Y. H. Chu and R. C. Kennicutt. Internal motions of hii regions and giant hii regions. *Astrophysics and Space Science*, 216:253–262, 1994. doi: 10.1007/BF00982502.
- [9] W. D. Cotton, J. J. Condon, and E. Arbizzani. Arcsecond positions of ugc galaxies. *The Astrophysical Journal Supplement Series*, 125:409–412, 1999. doi: 10.1086/313286.

- [10] G. de Vaucouleurs, A. de Vaucouleurs, H. G. JR. Corwin, R. J. Buta, G. Paturel, and P. Fouqué. Third reference catalogue of bright galaxies. *Springer–Verlag New–York Inc.*, 1991.
- [11] M. A. Dopita, L. Binette L., S. DÓdorico, and P. Benvenuti P. Radiative shock-wave theory. i. chemical abundance diagnostics and galactic abundance gradients. *Astrophysical Journal*, 276:653–666, 1984. doi: 10.1086/161653.
- [12] L. Drissen, J.-R. Roy, and A. F. J. Moffat. A search for wolf-rayet stars in active star forming regions of low mass galaxies: Gr8, ngc 2366, ic 2574, and ngc 1569. *The Astronomical Journal*, 106:1460–1470, 1993. doi: 10.1086/116739.
- [13] L. Drissen, J.-R. Roy, C. Roberts, D. Devost, and R. Doyon. The star formation history of the starburst region ngc 2363 and its surroundings. *The Astronomical Journal*, 119:688–704, 2000. doi: 10.1086/301204.
- [14] E. N. Ercan, E. Aktekin, N. Cesur, and A. Tumer. Optical and x-ray observational search for the possible supernova remnant candidates in the nearby galaxy ngc 1569. *Monthly Notices of the Royal Astronomical Society*, 481:2804–2812, 2018. doi: 10.1093/mnras/sty2456.
- [15] D. Monet et.al. Vizier online data catalog: A catalogue of astrometric standards. *VizieR Online Data Catalog*, 1252:0, 1998.
- [16] R. A. Fesen, F. Winkler, Y. Rathore, R. A. Downes, and D. Wallace. Optical imaging and spectroscopy of the galactic supernova remnants ctb 1 (g116.9+0.2), g116.5+1.1, and g114.3+0.3. *The Astronomical Journal*, 113:767–779, 1997. doi: 10.1086/118297.
- [17] R. A. Fesen, G. Rudie, A. Hurford, and A. Soto. Optical imaging and spectroscopy of the galactic supernova remnant 3c 58 (g130.7+3.1). *The Astrophysical Journal Supplement Series*, 174:379–395, 2008. doi: 10.1086/522781.

- [18] R. M. Gonzalez-Delgado, E. Perez, and G. Tenorio-Tagle. Violent star formation in ngc 2363. *Astrophysical Journal*, 437:239–261, 1994. doi: 10.1086/174992.
- [19] M. Hamuy, A. R. Walker, and N. B. Suntzeff. Southern spectrophotometric standards. i. *Publications of the Astronomical Society of the Pacific*, 104: 533–552, 1992. doi: 10.1086/133028.
- [20] M. Hamuy, N. B. Suntzeff, and S. R. Heathcote et al. Southern spectrophotometric standards. ii. *Publications of the Astronomical Society of the Pacific*, 106:566–589, 1994. doi: 10.1086/133417.
- [21] K. A. Herrmann, D. A. Hunter, and B. G. Elmegreen. Surface brightness profiles of dwarf galaxies. ii. color trends and mass profiles. *The Astronomical Journal*, 151:145–161, 2016. doi: 10.3847/0004-6256/151/6/145.
- [22] D. A. Hunter, B. G. Elmegreen, and H. van Woerden. Neutral hydrogen and star formation in the irregular galaxy ngc 2366. *The Astrophysical Journal*, 556:773–800, 2001. doi: 10.1086/321611.
- [23] S. D. Hyman, D. Calle, K. W. Weiler, C K. Lacey, S. D. Van Dyk, and R. Sramek. Radio continuum imaging of the spiral galaxy ngc 4258. *The Astrophysical Journal*, 551:702–711, 2001. doi: 10.1086/320231.
- [24] G. H. Jacoby, R. J. Quigley, and J. L. Africano. Two-dimensional spectrophotometry of planetary nebulae by ccd imaging. *Publications of the Astronomical Society of the Pacific*, 99:672–685, 1987. doi: 10.1086/132032.
- [25] A. E. Jaskot and M. S. Oey. The origin and optical depth of ionizing radiation in the "green pea" galaxies. *The Astrophysical Journal*, 766:91–113, 2013. doi: 10.1088/0004-637X/766/2/91.
- [26] V. E. Karachentseva, I. D. Karachentsev, and F. Boergen. Atlas of dwarf galaxies in the region of m 81 group. *Astronomy and Astrophysics, Suppl. Ser.*, 60:213–227, 1985.

- [27] R. Kennicutt, B. Balick, and T. Heckman. A remarkable h ii region complex in ngc 2366. *Astronomical Society of the Pacific, Publications*, 92:134–144, 1980. doi: 10.1086/130634.
- [28] R. Kennicutt, B. Balick, and T. Heckman. Multi-frequency radio continuum observations of dwarf irregular galaxies. *Astronomy and Astrophysics*, 161: 155–168, 1986.
- [29] C. Lacey and N. Duric. Cosmic-ray production and the role of supernovae in ngc 6946. *The Astrophysical Journal*, 560:719–729, 2001. doi: 10.1086/323048.
- [30] C. Lacey, N. Duric, and W. M. Goss. A survey of compact radio sources in ngc 6946. *The Astrophysical Journal Supplement Series*, 109:417–460, 1997. doi: 10.1086/312989.
- [31] J. H. Lee and M. G. Lee. A new optical survey of supernova remnant candidates in m31. *The Astrophysical Journal*, 786:130–147, 2014. doi: 10.1088/0004-637X/786/2/130.
- [32] I. Leonidaki, P. Boumis, and A. Zezas. A multiwavelength study of supernova remnants in six nearby galaxies - ii. new optically selected supernova remnants. *Monthly Notices of the Royal Astronomical Society*, 429:189–220, 2013. doi: 10.1093/mnras/sts324.
- [33] H.-H. Loose and T. X. Thuan. in star forming dwarf galaxies and related objects. *ed. D. Kunth, T. X. Thuan & J. T. T. Van (Éditions Frontières)*, 73, 1986.
- [34] J. Masegosa and M. Moles A. del Olmo. Spatial inhomogeneities in giant extragalactic hii regions. *Astronomy and Astrophysics*, 249:505–517, 1991.
- [35] P. Massey, K. Strobel, J. V. Barnes, and E. Anderson. Spectrophotometric standards. *Astrophysical Journal*, 328:315–333, 1988. doi: 10.1086/166294.

- [36] D. S. Mathewson and J. N. Clarke. Supernova remnants in the large magellanic cloud. *Astrophysical Journal*, 180:725–738, 1973. doi: 10.1086/152002.
- [37] D. M. Matonick and R. A. Fesen. Optically identified supernova remnants in the nearby spiral galaxies: Ngc 5204, ngc 5585, ngc 6946, m81, and m101. *The Astrophysical Journal Supplement Series*, 112:49–107, 1997. doi: 10.1086/313034.
- [38] F. Mavromatakis, P. Boumis, and E. V. Paleologou. Imaging and spectroscopy of the faint remnant g 114.3+0.3. *Astronomy and Astrophysics*, 383:1011–1017, 2002. doi: 10.1051/0004-6361:20011840.
- [39] G. Micheva, M. S. Oey, A. E. Jaskot, and B. L. James. Mrk 71/ngc 2366: The nearest green pea analog. *The Astrophysical Journal*, 845:165–177, 2017. doi: 10.3847/1538-4357/aa830b.
- [40] K. G. Noeske, N. G. Guseva, K. J. Fricke, and et al. Cometary blue compact dwarf galaxies. *Astrophysics and Space Science*, 277:487–487, 2000. doi: 10.1023/A:1012712012235.
- [41] D. E. Osterbrock and G. J. Ferland. Astrophysics of gaseous nebulae and active galactic nuclei. *2nd edn. University Science Books, Sausalito, CA*, University Science Books, 2006.
- [42] R. Pakmor, M. Kromer, S. Taubenberger, S. A. Sim, F. K. Ropke, and W Hillebrandt. Normal type ia supernovae from violent mergers of white dwarf binaries. *The Astrophysical Journal Letters*, 747:L10–L14, 2012. doi: 10.1088/2041-8205/747/1/L10.
- [43] R. Pakmor, M. Kromer, and V. Springel. Helium-ignited violent mergers as a unified model for normal and rapidly declining type ia supernovae. *The Astrophysical Journal Letters*, 770:L8–L14, 2013. doi: 10.1088/2041-8205/770/1/L8.
- [44] T. G. Pannuti, N. Duric, C. Lacey, W. M. Goss, C. G. Hoopes, R. A. M. Walterbos, and M. A. Magnor. An x-ray, optical, and radio search for

- supernova remnants in the nearby sculptor group sd galaxy ngc 300. *The Astrophysical Journal*, 544:780–804, 2000. doi: 10.1086/317238.
- [45] T. G. Pannuti, D. A. Swartz, N. Duric, and D. Urosevic. An x-ray, optical and radio search for supernova remnants in m81. *American Astronomical Society*, 200:3505, 2002.
- [46] T. G. Pannuti, E. M. Schlegel, and C. K. Lacey. A search for chandra-detected x-ray counterparts to optically identified and candidate radio supernova remnants in five nearby face-on spiral galaxies. *The Astronomical Journal*, 133:1361–1372, 2007. doi: 10.1086/510718.
- [47] G. Paturel, P. Dubois, C. Petit, and F. Woelfel. Comparison leda/simbad octobre 2002. catalogue to be published in 2003. *LEDA*, 2002.
- [48] P. Predehl and J. H. M. M. Schmitt. X-raying the interstellar medium: Rosat observations of dust scattering halos. *Astronomy and Astrophysics*, 500:459–475, 2009.
- [49] M. Relano, U. Lisenfeld, J. M. Vilchez, and E. Battaner. Distribution of extinction and star formation in ngc 1569. *Astronomy and Astrophysics*, 452:413–421, 2006. doi: 10.1051/0004-6361:20054607.
- [50] M. M. De Robertis, R. J. Dufour, and R. W. Hunt. A five-level program for ions of astrophysical interest. *Journal of the Royal Astronomical Society of Canada*, 81:195–220, 1987.
- [51] J.-R. Roy, J. Boulesteix, G. Joncas, and B. Grundseth. Superbubble blowout in the giant h II region ngc 2363? *Astrophysical Journal*, 367:141–148, 1991. doi: 10.1086/169609.
- [52] J.-R. Roy, M. Aube, M. L. McCall, and R. J. Dufour. The origin of broad emission lines in the extragalactic giant h II region ngc 2363. *Astrophysical Journal*, 386:498–505, 1992. doi: 10.1086/171035.

- [53] L. Searle, W. L. W. Sargent, and W. G. Bagnuolo. The history of star formation and the colors of late-type galaxies. *Astrophysical Journal*, 179:427–438, 1973. doi: 10.1086/151882.
- [54] R. A. Shaw and R. J. Dufour. Software for the analysis of emission line nebulae. *Publications of the Astronomical Society of the Pacific*, 107:896–906, 1995. doi: 10.1086/133637.
- [55] R. C. Smith, R. P. Kirshner, W. P. Blair, K. S. Long, and P. F. Winkler. Optical emission-line properties of m33 supernova remnants. *Astrophysical Journal*, 407:564–578, 1993. doi: 10.1086/172538.
- [56] K. R. Sokal, K. E. Johnson, R. Indebetouw, and P. Massey. The prevalence and impact of wolf-rayet stars in emerging massive star clusters. *The Astrophysical Journal*, 826:194–220, 2016. doi: 10.3847/0004-637X/826/2/194.
- [57] E. Sonbas, A. Akyuz, and S. Balman. An optical search for supernova remnants in the nearby spiral galaxy ngc 2903. *Astronomy and Astrophysics*, 493:1061–1065, 2009. doi: 10.1051/0004-6361:200810690.
- [58] E. Sonbas, A. Akyuz, S. Balman, and M. E. Ozel. A search for supernova remnants in the nearby spiral galaxy m 74 (ngc 628). *Astronomy and Astrophysics*, 517:A91, 2010. doi: 10.1051/0004-6361/200913858.
- [59] I. R. Stevens and D. K. Strickland. A rosat survey of wolf-rayet galaxies - ii. the extended sample. *Monthly Notices of the Royal Astronomical Society*, 301:215–230, 1998. doi: 10.1046/j.1365-8711.1998.02022.x.
- [60] S. Taubenberger, M. Kromer, R. Pakmor, G. Pignata, K. Maeda, S. Hachinger, B. Leibundgut, and W. Hillebrandt. O I $\lambda\lambda$ 6300-6364 Å in the nebular spectrum of a subluminescent type ia supernova. *The Astrophysical Journal Letters*, 775:L43–L47, 2013. doi: 10.1088/2041-8205/775/2/L43.
- [61] T. X. Thuan and Y. I. Izotov. High-ionization emission in metal-deficient blue compact dwarf galaxies. *The Astrophysical Journal Supplement Series*, 161:240–270, 2005. doi: 10.1086/491657.

- [62] T. X. Thuan, F. E. Bauer, and Y. I. Izotov. The x-ray properties of the cometary blue compact dwarf galaxies mrk 59 and mrk 71. *Monthly Notices of the Royal Astronomical Society*, 441:1841–1853, 2014. doi: 10.1093/mnras/stu716.
- [63] N. A. Tikhonov, B. I. Bilkina, I. D. Karachentsev, and Ts. B. Georgiev. Distance of nearby galaxies ngc 2366, ic 2574, and ngc 4236 from photometry of their brightest stars. *Astronomy and Astrophysics, Suppl. Ser.*, 89: 1–13, 1991.
- [64] E. Tolstoy, A. Saha, J. G. Hoessel, and K. McQuade. Variable stars in the irregular galaxy ngc 2366 (ddo 42). *The Astronomical Journal*, 110: 1640–1648, 1995. doi: 10.1086/117637.
- [65] M. M. Vučetić, D. Onić, N. Petrov, A. Čiprijanović, and M. Z. Pavlović. Optical observations of the nearby galaxy ngc 2366 through narrowband h α and [s II] filters. supernova remnants status. *Serbian Astronomical Journal*, 198:13–23, 2019. doi: 10.2298/SAJ190131003V.
- [66] H. Yang, E. D. Skillman, and R. A. Sramek. A kinematic search for supernova remnants in giant extragalactic h II regions. *The Astronomical Journal*, 107:651–661, 2019. doi: 10.1086/116885.

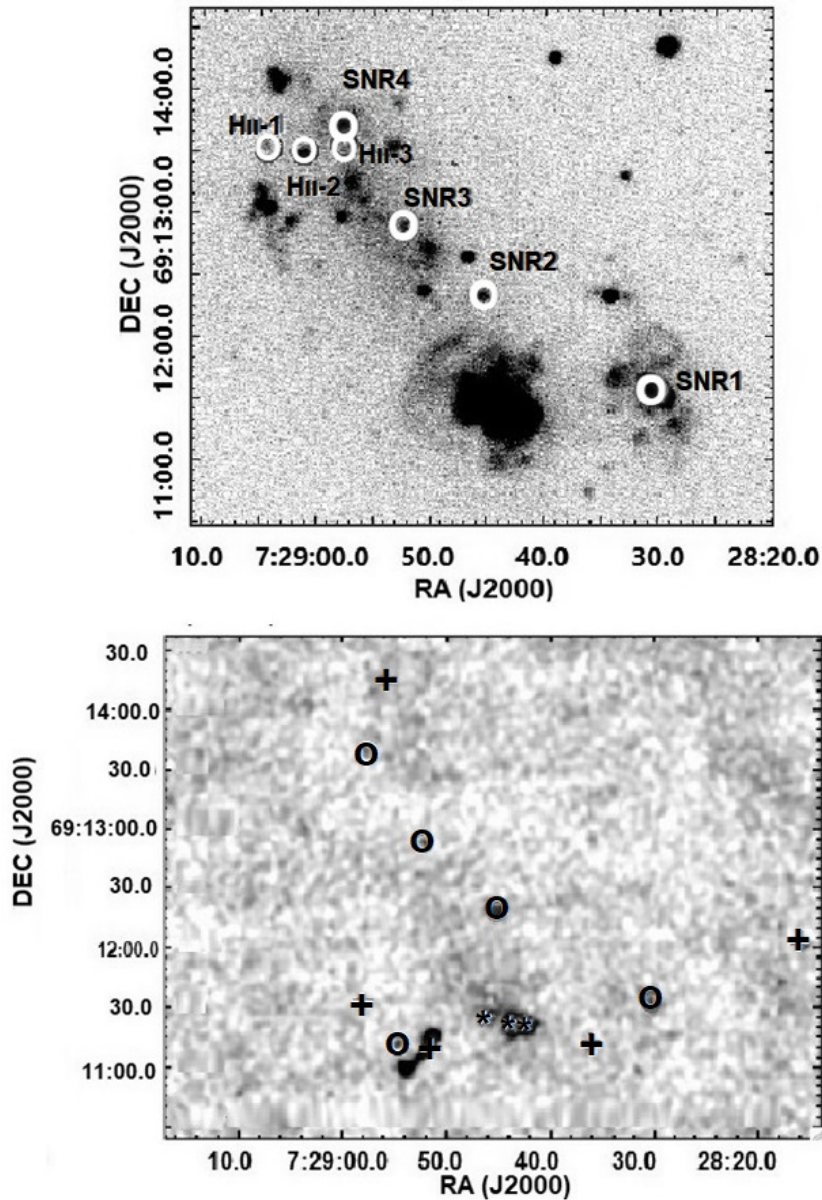


Figure 1: Top Panel: Combined RTT150 data: The H α image of NGC 2366 with J2000. Possible SNR candidates are given with thick white circles with our SNR1, SNR2, SNR3 and SNR4, which are matched with the radio SNR candidates of Chomiuk and Wilcots [7] are shown. Our HII regions are given with thin white circles HII-1, HII-2 and HII-3 are shown. Bottom Panel: Chomiuk and Wilcots [7] 20 cm radio map of NGC 2366, with J2000, where “+” indicates background galaxies, “circles” their SNR candidates and “*” signs are their HII regions.

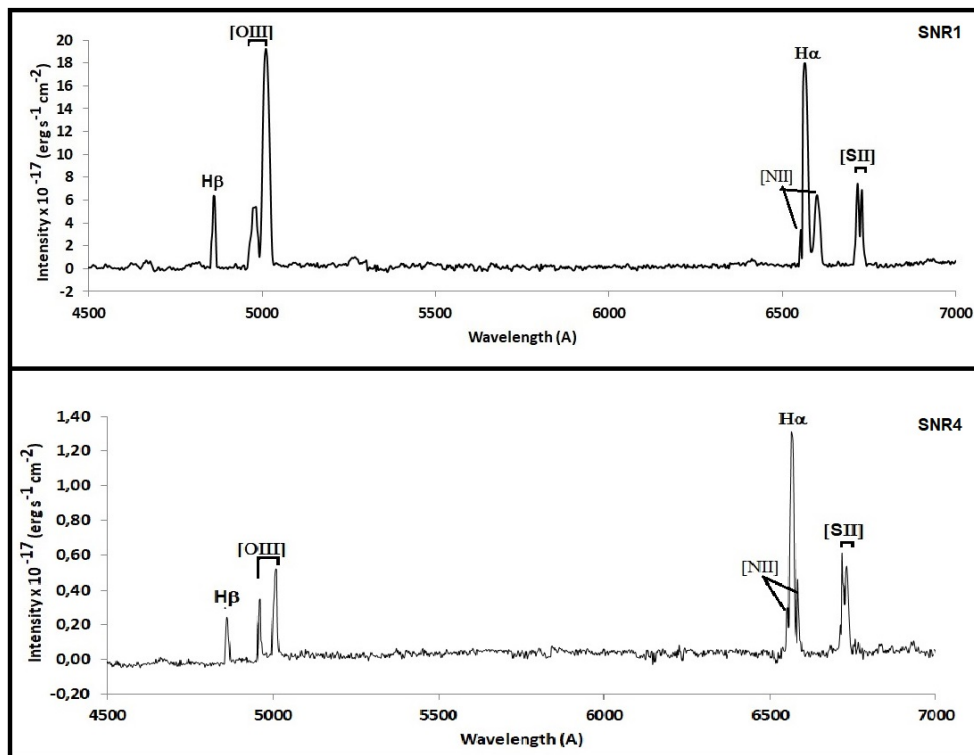


Figure 2: Spectra of SNR1 and SNR4 (Epoch 1) in $\lambda 4500\text{--}7000\text{ \AA}$ range. Its Balmer $H\alpha$ $\lambda 6563\text{ \AA}$, $H\beta$ $\lambda 4861\text{ \AA}$, forbidden lines $[O\text{ III}]\ \lambda\lambda 4959, 5007\text{ \AA}$, $[N\text{ II}]\ \lambda\lambda 6548, 6584\text{ \AA}$, $[S\text{ II}]\ \lambda\lambda 6717, 6731\text{ \AA}$ are shown.

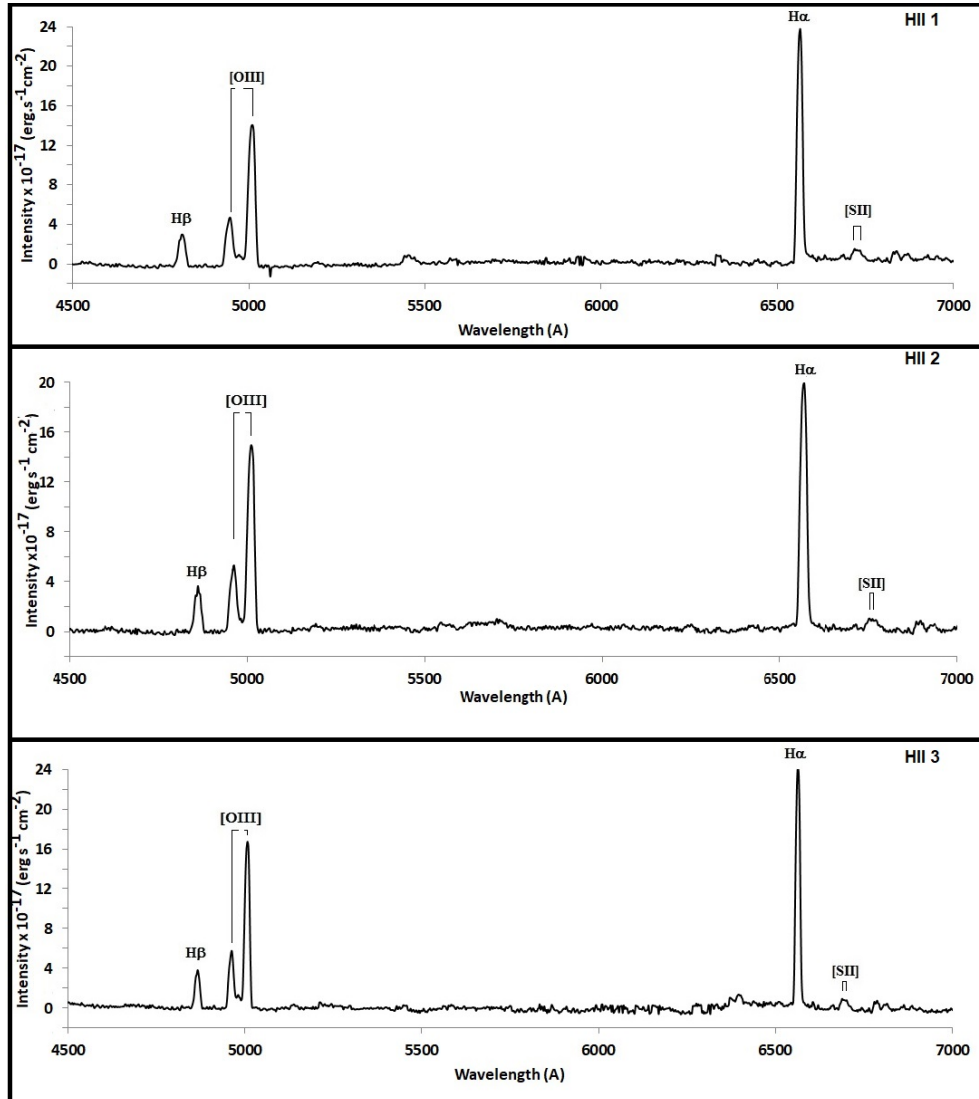


Figure 3: Spectra of HII region 1 (Epoch 1), 2 (Epoch 1) and 3 (Epoch 3) candidates in $\lambda 4500\text{--}7000 \text{ \AA}$ range.